Interdiffusion in a Tb|Y superlattice: an exploratory nuclear magnetic resonance study

1997 J. Phys.: Condens. Matter 9 6301

(http://iopscience.iop.org/0953-8984/9/29/015)

J. Phys.: Condens. Matter **9** (1997) 6301–6311. Printed in the UK PII: S0953-8984(97)82859-7

Interdiffusion in a Tb|Y superlattice: an exploratory nuclear magnetic resonance study

Y Li†, J W Ross†, M A H McCausland†, D St P Bunbury†, R C C Ward‡ and M R Wells‡

† The Schuster Laboratory, The University, Manchester M13 9PL, UK
‡ The Clarendon Laboratory, Oxford OX1 3PU, UK

Received 24 March 1997

Abstract. We have carried out an exploratory NMR study of interdiffusion at interfaces between epitaxially grown laminae of rare-earth metals. The system investigated was a terbium–yttrium superlattice grown by molecular-beam epitaxy at ∼270 °C. The NMR spectrum of ^{159}Tb shows satellites associated with Tb ions with different numbers of Y neighbours and therefore provides information about the yttrium concentration profile resulting from interdiffusion. Our data are interpreted in terms of a model based on thermally activated diffusion and which allows for the progressive decrease in σ, the RMS diffusion length, from the lowest to the highest interface. The diffusion coefficient, provisionally assumed to be independent of composition, is found to be $(9.0 \pm 0.6) \times 10^{-23}$ m^2 s^{-1} at the growth temperature.

1. Introduction

The study of metallic magnetism has taken a significant new turn with the advent of thin films and laminar structures with thicknesses controlled to within a few layers§. Such systems are interesting not only because they enhance our basic understanding of magnetic materials but also because of their potential applications for information storage. The structure and physics of rare-earth laminates grown by molecular-beam epitaxy (MBE) have been reviewed by Majkrzak *et al* (1991) and by Flynn and Salamon (1996).

Epitaxially grown laminae have excellent crystallinity, well-controlled thickness and, in the case of alloys, well-defined chemical composition. In the case of 3d metals, it is also possible to obtain atomically abrupt interfaces between chemically distinct laminae (see, for example, Lord *et al* 1993). In rare-earth laminates, however, there is a significant degree of interdiffusion at the interfaces, resulting in a concentration profile spread over several layers (Majkrzak *et al* 1991, McMorrow *et al* 1996).

Accurate characterization of interface quality is of the utmost importance not only for the interpretation of the magnetic behaviour of superlattices but also for the development of useful devices. It is also a prerequisite for the development of improved growth techniques. NMR has been used to study interfaces in the Cu|Co system (see, for example, Thomson *et al* (1994) and references therein), but to date the only information published on the quality of rare-earth interfaces is that derived from x-ray and neutron diffraction studies. Quantitative comparison of the published data is difficult because different authors adopt

§ Our terminology follows that defined by Graham *et al* (1993). In particular, 'layer' denotes a single atomic layer in the plane of the lamina.

0953-8984/97/296301+11$19.50

different models and different parameters to define the effective width of the interface. The analysis to be described in this paper is based on the one-dimensional diffusion equation. The fundamental parameter defining the concentration profile is the RMS diffusion length σ, but for mathematical convenience we shall define the effective width of the interface as $\lambda = \sqrt{2}\sigma$. On that basis, the values of λ deduced from the x-ray form factor measurements of Jehan *et al* (1993) and McMorrow *et al* (1996) for Ho|Y superlattices range from $1.5d$ to $7d$, where d is the distance between successive (0001) planes. The width and character of the interfaces in a given superlattice will of course depend on the rare-earth species involved and on the thermal history of the sample during and after the deposition process. We provisionally assume that interface widths for rare-earth–yttrium interfaces fall in the range quoted above. One factor that appears to have been ignored in previous studies is the spatial variation in λ entailed by the fact that the lower layers in a superlattice will have been exposed to elevated temperatures for a longer time than the upper ones.

Interface widths derived from diffraction measurements generally include surface roughness as well as interdiffusion, and it is difficult to separate the two (see McMorrow *et al* 1996). NMR spectra, on the other hand, reflect the local chemical composition and are insensitive to surface roughness unless interdiffusion is negligible. (The work of Thomson *et al* (1994) on the Cu|Co system shows that NMR spectra can reveal steps and other microscopic features on atomically abrupt interfaces.) The work to be described is an exploratory NMR study of interdiffusion between terbium and yttrium at the interfaces in a Tb|Y superlattice grown by MBE. It draws on results obtained in our recent study of transferred hyperfine interactions in epitaxial Tb:Y alloys (Li *et al* 1996). For the reasons outlined in the preceding paragraph, we include a substantial discussion of the nature of the diffusion profile as well as its relationship to the NMR spectrum.

2. Theory

Very little is known about the mechanism of diffusion in epitaxially grown rare earths. The most likely process is thermally activated motion of vacancies, but we have no quantitative information about the activation energies for the creation of vacancies or for their subsequent migration. Also unknown are the relative probabilities for different chemical species to occupy a given vacancy. In the absence of such information we are obliged to adopt the simplest assumptions consistent with the available data. In particular, we provisionally assume that diffusion rates are independent of the local composition and of the diffusing species. We shall however allow for the fact that the extent of interdiffusion at any position in a superlattice is determined by its thermal history.

For the sake of generality, and with future applications in mind, we consider a composite system consisting of two metals A and B. We assume only that both metals have HCP structure and similar lattice parameters. To avoid repetition, 'neighbour' will denote a *nearest* neighbour except where stated otherwise. In order to make contact with our NMR data (to be described in section 4) we need to calculate $R(n)$, the relative numbers of A ions with n B neighbours under various assumptions about the spatial variation of the B concentration. Explicitly,

$$R(n) = \mathcal{N}(n)/\mathcal{N}(0)$$

where $\mathcal{N}(n)$ is the total number of A ions with n B neighbours in the entire sample.

2.1. The special case of a uniform alloy

Consider a uniform alloy $A_{1-x}B_x$ in which the fractional concentration of B is x. The probability of finding a given A ion with n B neighbours is

$$P(N, n, x) = \frac{N!}{n!(N-n)!}x^n(1-x)^{(N-n)} \tag{1}$$

where N, the total number of neighbours, is 12 for HCP metals. It follows that

$$R(n) = R(n, x) = \frac{P(12, n, x)}{P(12, 0, x)}. \tag{2}$$

This expression underlies the analysis of our NMR spectra in Tb:Y alloys (Li *et al* 1996).

2.2. Non-uniform alloys

Consider now a non-uniform HCP alloy, such as the superlattice under discussion, in which the concentration of B varies along the c-direction. Thus $x = x(z)$, where the z-axis is taken parallel to c. A representative A atom in the kth layer has three distinct sets of neighbours: three in layer $(k-1)$, six in layer k, and three in layer $(k+1)$. The probabilities of finding p, q and r B atoms in each of these layers are respectively $P(3, p, x_{k-1})$, $P(6, q, x_k)$ and $P(3, r, x_{k+1})$ where $x_k = x(z_k)$. It follows that the probability for an A ion in layer k to have n B neighbours is

$$P_k(n) = \sum_{[p,q,r]} P(3, p, x_{k-1})P(6, q, x_k)P(3, r, x_{k+1}) \tag{3}$$

where p and r run from 0 to 3, q runs from 0 to 6 and the sum over p, q and r is restricted to terms such that $p+q+r = n$. The relative numbers of A ions in the entire sample with n B neighbours are then obtained by summing the $P_k(n)$ over all layers in the laminate:

$$R(n) = \sum_k P_k(n) \Big/ \sum_k P_k(0). \tag{4}$$

These numbers clearly depend on the form of the concentration profile $x(z)$ and form a sequence which, in general, will differ from that given by equation (2).

2.3. The concentration profile in the neighbourhood of a single interface

Consider a single interface between two laminae, A and B, both of which are thick in comparison with λ, a parameter characteristic of the width of the interdiffusion region. We take the origin ($z = 0$) at the interface, with $z < 0$ and $z > 0$ for A and B respectively. A qualitative description of the concentration profile for species B can be given by any function $x(z)$ which increases smoothly from zero for $z \ll -\lambda$ to unity for $z \gg \lambda$. Jehan *et al* (1993), for example, use a profile based on a hyperbolic tangent. Following Kwo *et al* (1985) we use an expression based on the error function erf which, unlike tanh, has a physical basis in the one-dimensional diffusion equation

$$\frac{\partial x}{\partial t} = D\frac{\partial^2 x}{\partial z^2}. \tag{5}$$

If the diffusion coefficient D is independent of concentration this leads, in the case under discussion, to the concentration profile

$$x(z) = \frac{1 + \mathrm{erf}(z/\lambda)}{2} \tag{6}$$

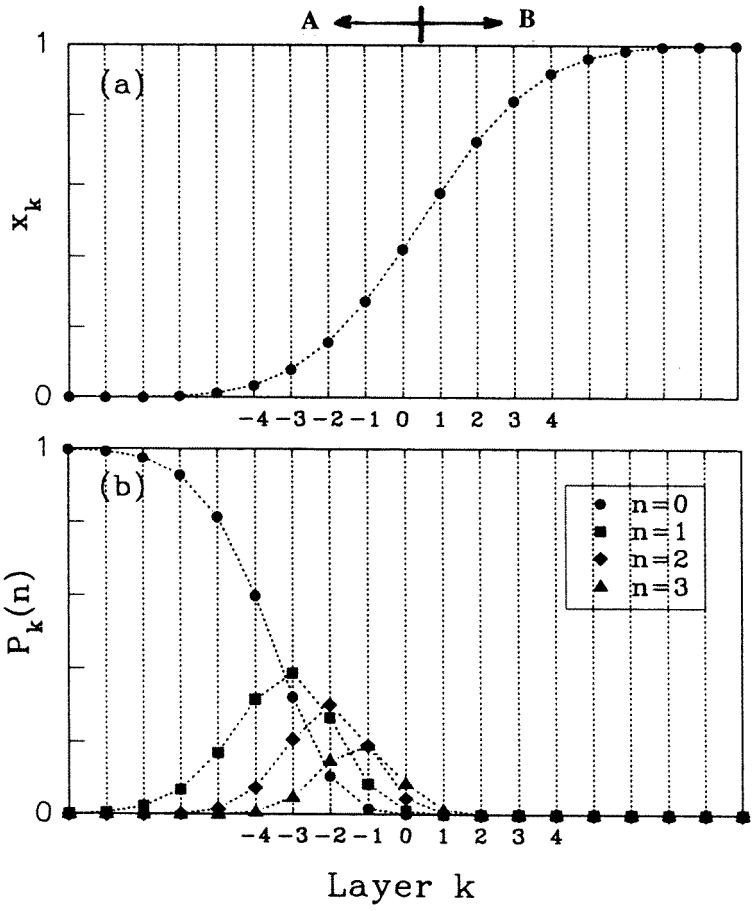

Figure 1. (a) The concentration profile of metal B in the vicinity of an A|B interface when $\sigma/d = 2.5$. (b) Probabilities $P_k(n)$ for an A atom in layer k to have n B neighbours.

where λ is related to σ, the RMS diffusion length, and to the diffusion coefficient D by $\lambda = \sqrt{2}\sigma = 2\sqrt{Dt}$ where t is the duration of the diffusion process (see, for example, Crank 1975). We assume, for simplicity, that the sample has been grown at a constant elevated temperature T_G and subsequently quenched abruptly to a temperature at which the diffusion rate is insignificant. Thus $D = D(T_G)$ may be treated as a constant. Allowance for a finite cooling rate will be considered in section 2.5.

The calculation of $R(n)$ follows straightforwardly from equations (3) and (4) by setting

$$x_k = \frac{1 + \operatorname{erf}[(k - \frac{1}{2})d/\lambda]}{2} \tag{7}$$

where $d = c/2$ is the distance between successive (0001) layers. We count k from the first B layer to the right of the interface which, by definition, is midway between the last A layer and the first B layer. Thus $z_k = (k - \frac{1}{2})d$. Figure 1 shows the concentration profile and the corresponding values of $P_k(n)$ for $\sigma = 2.5d$ ($\lambda \cong 3.54d$). In order to obtain a finite value for $\sum_k P_k(0)$ and hence for the $R(n)$ we must assume a finite number, N_A, of A layers. For the purpose of illustration, we take $N_A = 40$. This gives $R(n) = 0.0374$ for $n = 1$, 0.0236 for $n = 2$ and 0.0138 for $n = 3$. In figure 2 we plot $R(n)$ as a function of σ/d. In

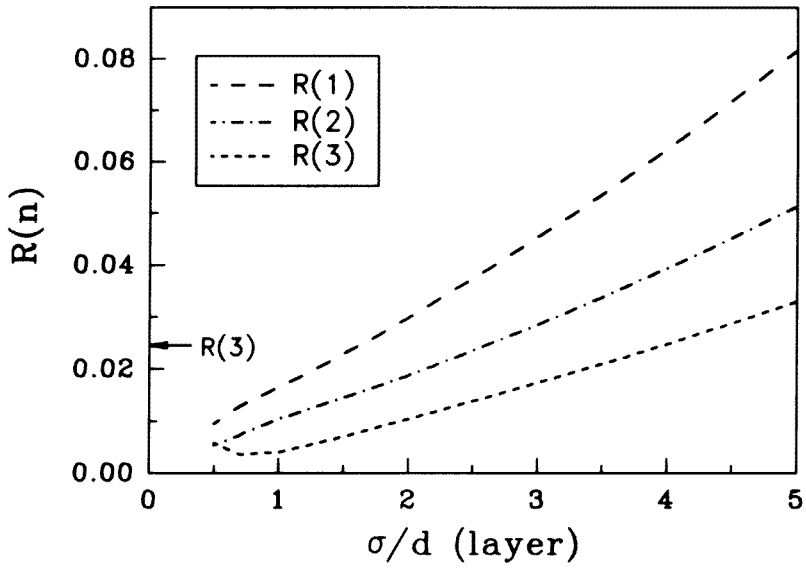

Figure 2. Relative probabilities $R(n)$ for an A atom to have n B neighbours as functions of σ/d. The total number of A atoms corresponds to 40 layers.

the limit $\sigma/d \to 0$ all $R(n)$ vanish except $R(3)$, which becomes $1/(N_A - 1)$ ($\cong$0.0256 in the case under discussion).

Bearing in mind the discrete nature of the crystal lattice and the fact that the diffusion process takes place by a finite number of discrete jumps, we may expect the continuum model of diffusion (equations (5) to (7)) to break down when σ/d, and hence the average number of jumps during the diffusion process, is small. We have therefore tested the predictions of the continuum model against those obtained from a Monte Carlo calculation in which the diffusion process is modelled by the random motion of vacancies into which A or B neighbours can jump with equal *a priori* probability. We find that the continuum approximation remains adequate down to $\sigma/d \sim 1.5$ ($\lambda \sim 2d$).

2.4. Laminae of finite thickness

If the thicknesses of the laminae in a superlattice are not large compared to λ, a significant number of A atoms may pass through the B laminae, and conversely. In that case it is necessary to superimpose two or more functions of the form (7) to obtain the resultant concentration profile. In principle, one such function may be required for every interface in the superlattice. In the present work we are concerned with a superlattice consisting of units $A_{40}|B_{20}$. Assuming, as before, that $1.5d < \lambda < 7d$ we may neglect penetration of the A laminae by B, but not conversely. We may therefore treat each B lamina as a slab of finite thickness W ($=20d$ in the case under discussion) between two effectively infinite slabs of A. Taking the local origin at the centre of the B lamina, we now obtain a two-term expression for the local concentration profile:

$$x(z) = \frac{\operatorname{erf}[(W/2 + z)/\lambda] + \operatorname{erf}[(W/2 - z)/\lambda]}{2}. \tag{8}$$

(See Crank 1975.) A discrete version of this expression will be applied to the analysis of our NMR data in section 4.

2.5. Spatial variation of the diffusion length

Rare-earth superlattices are normally grown at an elevated temperature (typically >250 °C) and then allowed to cool to ambient temperature. Thermally activated interdiffusion will therefore be more extensive at the bottom of the superlattice than at the top and appropriate allowance should be made for the variation in λ from one interface to another. The form of the variation for a given superlattice will depend on the details of its thermal history. In the special case that the superlattice is grown at a constant temperature T_G and then rapidly quenched to a temperature at which the diffusion rate is negligible, the RMS diffusion length for a given interface is given by $\sigma_I = \sqrt{2D_G t_I}$ where $D_G = D(T_G)$ and t_I is the time for which interface I was maintained at T_G. To allow for additional diffusion during the cooling process, we write

$$\sigma_I = \sqrt{2D_G t_I^{eff}} \tag{9}$$

where $t_I^{eff} = t_I + \Delta t$ and Δt is approximated by

$$\Delta t \cong (D_G)^{-1} \int D[T(t)]\ \mathrm{d}t = \exp(E_a/kT_G) \int \exp\{-E_a/[kT(t)]\}\ \mathrm{d}t \tag{10}$$

where E_a is the activation energy for the diffusion process and the integral is taken over an appropriately defined cooling period.

3. Experimental procedures

The superlattice SL658 used in this work was grown at the LaMBE facility in Oxford on a 10 mm × 12 mm niobium-coated sapphire substrate, following the procedures developed by Kwo *et al* (1985). It consists of 25 repeats of ($Tb_{40}|Y_{20}$) sandwiched between a 300-layer seed lamina of yttrium and a 70-layer protective cap of yttrium (see figure 3). The crystallographic *c*-axis is parallel to the growth direction; the *a*- and *b*-axes are respectively parallel to the 12 mm and 10 mm edges of the substrate. The lattice parameters of Y and Tb agree to within 1%; for the purposes of the present work we assume the average interlayer spacing $d = c/2 \cong 0.286$ nm.

The superlattice and cap were grown at 270 °C. The deposition rate was constant at ∼0.174 layers per second. The heater was switched off as soon as the top layer was complete. The decay in temperature conformed closely to a Newtonian cooling curve with a time constant of ∼30 minutes.

For the NMR measurements the sample was mounted on an inside wall of a tunable rectangular TE_{011} resonator situated within a superconducting solenoid and immersed in liquid helium. The orientation of the substrate was such that both the RF and DC fields were parallel to the crystallographic *a*- and *b*-axes, respectively. Since the direction of spontaneous magnetization for terbium is along a *b*-axis, the DC and RF fields were respectively parallel and perpendicular to the magnetization. The measurements were made on the 100%-abundant ^{159}Tb isotope with a high-speed spin-echo spectrometer similar to that described by Carboni *et al* (1989). They were carried out at a temperature of 1.4 K, in fields up to 4 T and at frequencies between 2300 MHz and 3900 MHz. The estimated microwave skin depth in that frequency range is ∼3 μm, considerably greater than the total thickness of the superlattice (∼0.5 μm).

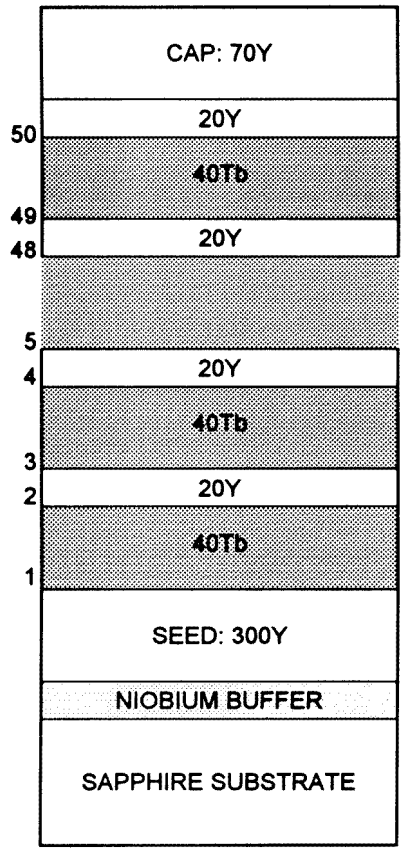

Figure 3. The stacking sequence in the superlattice $[Y_{300}|(Tb_{40}|Y_{20})_{25}|Y_{70}]$ (not to scale). The numbers on the left label the Tb|Y interfaces I_1 to I_{50}.

4. Results and analysis

The three-line quadrupole-split NMR spectra obtained from the superlattice are characteristic of ^{159}Tb and are qualitatively similar to those previously obtained for epitaxially grown Tb:Y alloys (Li *et al* 1996). The spectra taken in finite fields are shifted upwards in frequency by $\cong$10 MHz T^{-1}, which corresponds closely to the gyromagnetic ratio of ^{159}Tb. This, together with the absence of a perceptible field dependence of the quadrupole splitting, indicates that crystal-field quenching of the parent Tb moment is insignificant. In what follows we shall be concerned only with the zero-field spectrum, in which the satellite structure is more sharply resolved than it is in the spectra obtained in higher fields. The central line is shown in figure 4, together with the corresponding line for a $Tb_{0.95}Y_{0.05}$ alloy.

Li *et al* (1996) have shown that transferred hyperfine interactions in Tb:Y alloys are dominated by isotropic contributions from the 12 nearest neighbours. The satellite structure shown in figure 4(a) arises from Tb ions with $n = 0, 1, 2$ and 3 Y ions in the nearest-neighbour shell. The increase in satellite width with n is caused by the anisotropy of the local dipolar field, an effect also apparent in the superlattice spectrum (figure 4(b)). The separation between successive satellites ($\cong$ 12.5 MHz) is almost the same in the two systems. The downward shift ($\sim$4 MHz) of the satellites in figure 4(b) with respect to those

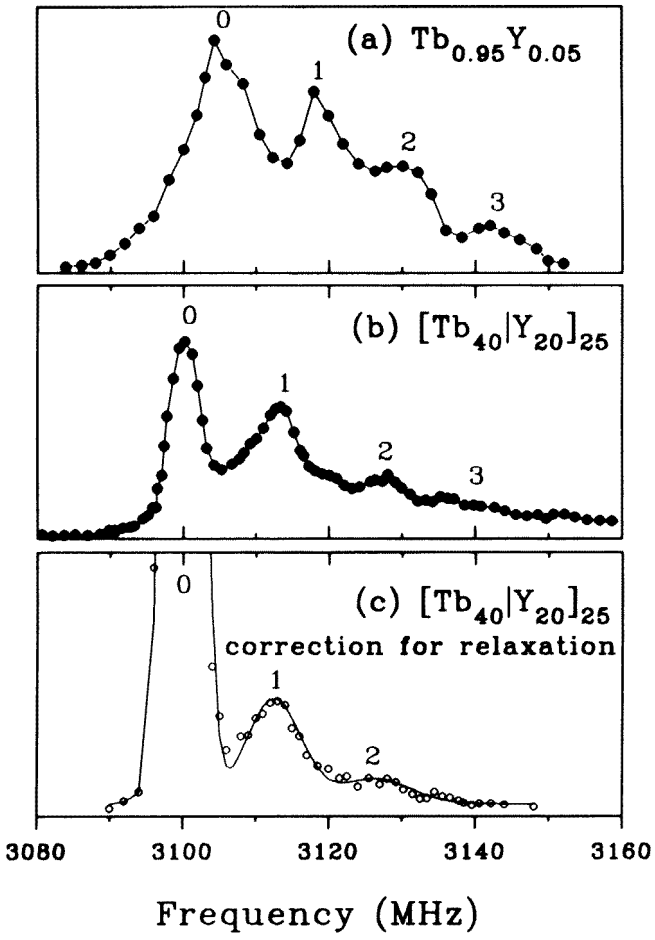

Figure 4. The central NMR lines of ^{159}Tb at 1.4 K and in zero field, (a) in the epitaxially grown alloy $Tb_{0.95}Y_{0.05}$; (b) in the superlattice $[Y_{300}|(Tb_{40}|Y_{20})_{25}|Y_{70}]$; (c) as in (b), after correction for relaxation. The lines are labelled by the numbers n of Y neighbours.

in figure 4(a) is consistent with the fact that the average dipolar field in the superlattice is ~0.3 T smaller than that in the alloy.

It is clear that the satellite structure in the superlattice has the same origin as that in the alloy. It follows at once that there must be some degree of interpenetration between the Tb and Y laminae. If the interfaces were abrupt, there would be only two classes of Tb ions: those in the interior of the Tb laminae, for which $n = 0$, and those at the interface, for which $n = 3$, giving a single satellite about 38 MHz above the main line.

In what follows we use the relative intensities of the satellites to determine the relative numbers of Tb ions with different values of n and hence to quantify the extent of interdiffusion. The first step is to correct the raw data for the effects of nuclear relaxation, which varies markedly across the satellite pattern. Representative values of T_1 and T_2 are given in table 1. The spectrum shown in figure 4(c) is obtained by extrapolating to zero pulse separation the spin-echo decays measured at numerous frequencies. The extrapolated spectrum was then fitted to a set of three Gaussians, the areas of which are proportional to

Table 1. Summary of NMR data for Tb ions with $n = 0, 1$ and 2 Y neighbours at 1.4 K and in zero field: centre frequencies ν; longitudinal and transverse relaxation times T_1 and T_2 at frequencies ν; and areas $R(n)$ of satellites relative to $n = 0$ after correction for relaxation.

n	0	1	2
ν (MHz)	3100	3113	3126
T_1 (μs)	22	36	—
T_2 (μs)	0.5	2.5	3.2
$R(n)$	1	0.120 ± 0.005	0.055 ± 0.015

the numbers $\mathcal{N}(n)$ of Tb ions with $n = 0, 1$ and 2 Y neighbours in the entire superlattice. The experimentally determined values of $R(n) = \mathcal{N}(n)/\mathcal{N}(0)$ are given in table 1. They are related to the yttrium concentration distribution by equations (3) and (4). It remains to relate the x_k to the diffusion coefficient.

Referring to figure 3, we observe that interfaces I_1 and I_{50} are well separated from the others. Their concentration profiles may therefore be described by the single-erf expression (equation (7)), with appropriate values of $\lambda = \lambda_I = \sqrt{2}\sigma_I$ obtained from equations (9) and (10). In the absence of numerical data on activation energies for diffusion in epitaxially grown rare earths we have taken $E_a \sim 2.9$ eV, a figure based on data for bulk erbium and yttrium (see Dariel 1978). This, together with the experimentally determined cooling curve, gives $\Delta t \sim 70$ s. (The integral in equation (10) was truncated at a time such that the diffusion rate had fallen by ~8 orders of magnitude.) Adding Δt to the t_I derived from the known growth rate we obtain $t_1^{eff} = 9070 \pm 100$ s and $t_{50}^{eff} = 590 \pm 20$ s. It follows from equation (9) that there is a fourfold increase in σ from the top to the bottom of the superlattice.

Following the discussion in section 2.4, we group the remaining interfaces into pairs (I_2, I_3), (I_4, I_5), ..., (I_{48}, I_{49}) and describe the concentration profile for each pair by an expression equivalent to equation (8), with $W_B = W_Y = 20d$ and $z = z_k = (k - \frac{1}{2})d$. (We set $k = 1$ for the first layer on the positive-z side of the local origin, which is taken at the centre of the Y lamina and is therefore midway between two layers.) Thus

$$x_k = \frac{\operatorname{erf}[(9.5 + k)d/\lambda] + \operatorname{erf}[(10.5 - k)d/\lambda]}{2}. \tag{11}$$

The appropriate values of t_I^{eff} and hence of λ are calculated as indicated in the preceding paragraph, except that we assign a common value of λ to each pair. (The variation in λ across a single yttrium lamina is insignificant.)

The values of x_k, and hence of $P_k(n)$ (see equation (3)) for every layer in the superlattice, are now determined in terms of D_G. $R(n)$ is obtained as a function of D_G by summing over all layers. The results are plotted in figure 5. The values of D_G derived from the experimental data on $R(1)$ and $R(2)$ (table 1) are respectively $(11.2 \pm 0.8) \times 10^{-4}\, d^2\ \mathrm{s}^{-1}$ and $(6.5 \pm 3.1) \times 10^{-4}\, d^2\ \mathrm{s}^{-1}$. The weighted mean of these figures is $D_G = (11.0 \pm 0.7) \times 10^{-4}\, d^2\ \mathrm{s}^{-1} = (9.0 \pm 0.6) \times 10^{-23}\ \mathrm{m}^2\ \mathrm{s}^{-1}$. The corresponding values of σ range from $(1.1 \pm 0.2)d$ for the highest interface I_{50} to $(4.3 \pm 0.2)d$ for the lowest interface I_1. The average value of σ over all fifty interfaces is $(3.0 \pm 0.1)d$.

We comment as follows. First, the RMS diffusion lengths for the top five interfaces are within the regime where the continuum model becomes slightly inaccurate (see section 2.3). This however contributes a negligible error to the calculation of the diffusion coefficient. Second, the values of D_G derived from the data for $n = 1$ and $n = 2$ differ by ~1.5 standard deviations. This suggests that the true concentration profile for yttrium may differ from that

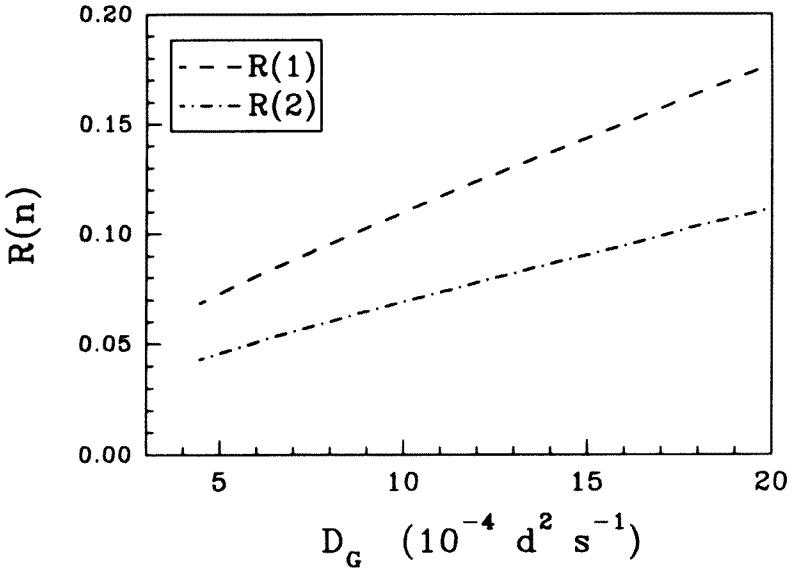

Figure 5. Relative probabilities $R(n)$ for a Tb atom to have n Y neighbours in the superlattice $[Y_{300}|(Tb_{40}|Y_{20})_{25}|Y_{70}]$ as functions of the diffusion coefficient D_G, expressed in units of d^2 s^{-1} where d is the interlayer spacing.

derived from our simple diffusion model. Our NMR data for $n = 1$ and $n = 2$ come, on average, from regions of different chemical composition (see figure 1). We tentatively suggest that the discrepancy may be explained in terms of a diffusion coefficient that varies with the local yttrium concentration. Given the differences between Y and Tb in atomic mass and in chemistry, a variation of this sort is inherently plausible. However, quantification of the effect will require more extensive measurements than those reported here.

5. Conclusions

Our exploratory study of a Tb|Y superlattice has demonstrated the potential of NMR to provide information about chemical interdiffusion independently of surface roughness and other factors which contribute to interface profiles obtained from x-ray and neutron diffraction measurements. We have also drawn attention to the spatial variation in diffusion lengths implicit in any model based on thermally activated diffusion, an effect which appears to have been ignored in the analysis of diffraction measurements. This is not a small effect: in the 25-repeat superlattice studied in the present work the RMS diffusion length increases by a factor of $\sim$4 from the top to bottom. Published values of σ derived from diffraction experiments must, presumably, be some sort of average over the entire superlattice. It would be interesting to analyse measured form factors using a model that allows for spatial variation in interface widths.

In this paper we have used the simplest possible model of the diffusion process. In particular, we have assumed (i) that the diffusion coefficient is independent of the local composition and (ii) that Y and Tb ions have equal mobilities. Our results suggest that (i) may require modification. They do not at present throw any light on (ii). That would require complementary measurements on ^{89}Y, for which the resonance frequency falls well

below the range of our microwave spectrometer.

There remains a great deal to be learnt about the systematics and mechanisms of interdiffusion in epitaxially grown rare-earth superlattices. We intend to follow up the work described here by further measurements on Tb|Y and related superlattices with different thicknesses and periodicities, and with different thermal histories. This should provide useful information on activation energies, for which no data are currently available other than those obtained for conventionally grown rare-earth crystals. Complementary NMR measurements on other nuclear species, and particularly on ^{89}Y, would be invaluable.

Acknowledgment

This work was supported by the UK Engineering and Physical Sciences Research Council.

References

Carboni C, Mackenzie I S and McCausland M A H 1989 *Hyperfine Interact.* **51** 1139

Crank J 1975 *The Mathematics of Diffusion* (Oxford: Clarendon)

Dariel M P 1978 *Handbook on the Physics and Chemistry of Rare Earths* vol 1, ed K A Gschneidner Jr and L Eyring (Amsterdam: Elsevier) ch 12

Flynn C P and Salamon M B 1996 *Handbook on the Physics and Chemistry of Rare Earths* vol 22, ed K A Gschneidner Jr and L Eyring (Amsterdam: Elsevier) ch 147

Graham R G, Ross J W, Bunbury D St P, McCausland M A H, Ward R C C and Wells M R 1993 *J. Phys.: Condens. Matter* **5** L647

Jehan D A, McMorrow D F, Cowley R A, Ward R C C, Wells M R, Hagmann N and Clausen K N 1993 *Phys. Rev.* B **48** 5594

Kwo J, Gyorgy E M, McWhan D B, Hong M, DiSalvo F J, Vettier C and Bower J E 1985 *Phys. Rev. Lett.* **55** 1402

Li Y, Ross J W, McCausland M A H, Bunbury D St P, Wells M R and Ward R C C 1996 *J. Phys.: Condens. Matter* **8** 11 291

Lord J S, Kubo H, Riedi P C and Walker M J 1993 *J. Appl. Phys.* **73** 6381

Majkrzak C F, Kwo J, Hong M, Yafet, Gibbs D, Chien C L and Bohr J 1991 *Adv. Phys.* **40** 99

McMorrow D F, Swaddling P P, Cowley R A, Ward R C C and Wells M R 1996 *J. Phys.: Condens. Matter* **8** 6553

Thomson T, Riedi P C and Greig D 1994 *Phys. Rev.* B **50** 10 319